Chemometrics-assisted spectroscopic methods for rapid analysis of combined anti-malarial tablets

Chemometrics-assisted spectroscopic methods for rapid analysis of combined anti-malarial tablets

Panawan Pruksapha [a,b], Putthiporn Khongkaew [c], Chaweewan Suwanvecho [a], Nantana Nuchtavorn [a], Chutima Phechkrajang [a], Leena Suntornsuk [a,*]

[a] Department of Pharmaceutical Chemistry, Faculty of Pharmacy, Mahidol University, Bangkok, Thailand
[b] The Government of Pharmaceutical Organization (GPO), Bangkok, Thailand
[c] Department of Pharmaceutical Chemistry, Faculty of Pharmaceutical Science, Burapha University, Chonburi, Thailand

Abstract

Combination of piperaquine (PQ) (320 mg) and dihydroartemisinin (DHA) (40 mg) is an anti-malarial formulation, which is recommended by World Health Organization (WHO). Simultaneous analysis of PQ and DHA can be problematic due to the lack of chromophores or fluorophores in DHA molecule. Whereas PQ possesses strong UV absorption and it presents in 8 times of DHA contents in the formulation. In this study, two spectroscopic methods, Fourier transform infrared (FTIR) and Raman spectroscopy, were developed for the determination of both drugs in combined tablets. The FTIR and Raman spectra were recorded in the attenuate total reflectance (ATR) and scattering modes, respectively. The original and pretreated spectra from FTIR and handheld-Raman were subjected to Unscrambler® program to construct partial least squares regression (PLSR) model comparing with references values obtained from high performance liquid chromatography (HPLC)-UV method. The optimal PLSR models of PQ and DHA from FTIR spectroscopy were obtained from orthogonal signal correction (OSC) pretreatment at the wavenumbers 400—1,800 cm^{-1} and 1,400—4,000 cm^{-1}, respectively. For Raman spectroscopy of PQ and DHA, the optimal PLSR models were obtained from standard normal variate (SNV) pretreatment at the wavenumbers 1,200—2,300 cm^{-1} and OSC pretreatment at the wavenumber 400—2,300 cm^{-1}, respectively. Determination of PQ and DHA in tablets from the optimum model was compared with HPLC-UV method. Results were not significantly different at 95% confidence limit (p-value >0.05). The chemometrics-assisted spectroscopic methods were fast (1—3 min), economical and less labor intensive. Moreover, the handheld Raman spectrometer is portable and can be utilized for onsite analysis to facilitate the detection of counterfeit or substandard drugs at ports of entry.

Keywords: Chemometrics, Dihydroartemisinin, Fourier transform infrared spectroscopy, Piperaquine, Raman spectroscopy

1. Introduction

Malaria is an endemic disease that affects billions of people worldwide, in 2020 only, 409,000 deaths were reported [1]. *Plasmodium falciparum* is the most prevalent parasite for malaria cases. Artemisinin and its derivatives in combination with other drugs are widely prescribed because of their rapid action and efficacy against multi-drug resistance of *P. falciparum*. Oral monotherapy, therefore, is withdrawn from all treatments since it promote drug resistance [1,2]. Anti-malarial drugs should be procured based on the guidelines for the treatment of malaria using WHO Model List of Essential Medicines [2]. Fixed-dose combined formulations are preferred to prevent drug resistance and at least two effective anti-malarial drugs with different mechanisms of actions should be treated for all episodes of malaria. Except for pregnant women in the first trimester, artemisinin-based combination therapies are recommended for the treatment of uncomplicated *P. falciparum* malaria [2].

Piperaquine (PQ) is a bisquinoline anti-malarial drug, which is available as water-soluble tetraphosphate salt [3] (Fig. 1 (A)). PQ is used for prophylaxis until the emergence of resistance and serves as a partner drug in artemisinin-based combination
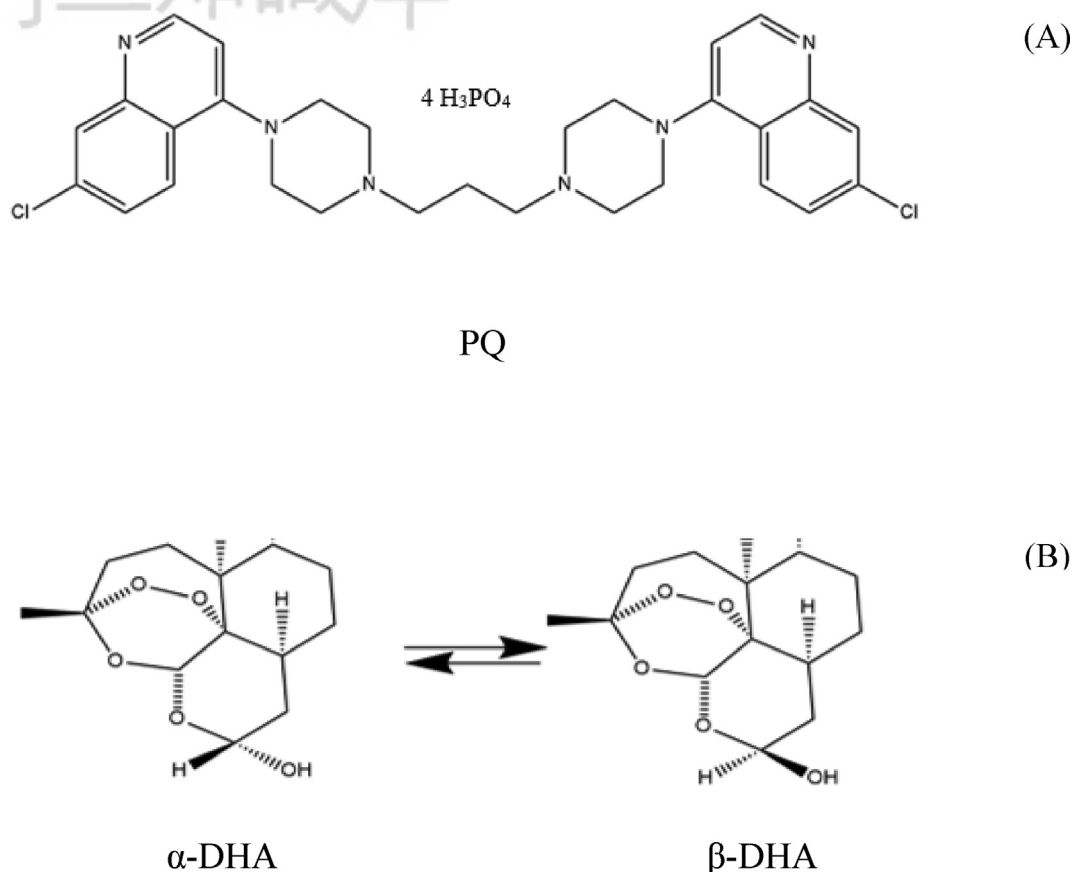
(A)

PQ

(B)

α-DHA   β-DHA

Fig. 1. Chemical structures of (A) PQ tetraphosphate, (B) the two interconverting epimers of DHA (left: α-dihydroartemisinin and right: β-dihydroartemisinin).

therapy (ACT) (i.e. dihydroartemisinin (DHA) [4,5]. DHA is a semi-synthetic derivative of artemisinin, also known as dihydroqinghaosu or artenimol. In solution, DHA can convert the lactone carbonyl group at C10 providing two lactol hemiacetal epimers, namely α-DHA (10 S-epimer) and β-DHA (10 R-epimer) (Fig. 1 (B)) depending on buffer, pH and solvent polarity [6,7]. Combination of PQ (320 mg) and DHA (40 mg) is recommended for the treatment of uncomplicated *P. falciparum* malaria in Thailand. However, low quality or substandard drugs are still found in some regions, which increases incidence of morbidity, mortality and drug resistance in malarial therapy [4,5].

Major problems for the assays of PQ and DHA include low water solubility and poor stability. Moreover, DHA lacks of chromophores and the detection at low wavelength is more susceptible to interference from solvents and sample matrices. On the other hand, PQ has strong UV absorption peaks at wavelengths 225, 239 and 340 nm [5] and it presents in 8 times of DHA contents in the combined formulations. Official methods for the quantitation

of PQ and DHA are not available in pharmacopeias, whereas the World Health Organization (WHO) recommends high performance liquid chromatography (HPLC) for DHA assay, which presents in α- and β-forms [7]. From literature searches, analyses of PQ are performed by HPLC method [8] and capillary electrophoresis [9]. Only few publications on assays of the combined formulation are published. For example, HPLC with UV detection [10] and tandem mass spectrometry (MS) [11] were proposed for the assays of PQ and DHA in plasma. HPLC-MS was also developed for the quantitation of both drugs in combined tablets [12]. In another work, HPLC was proposed for analyses of PQ and DHA in bulk, but applications in pharmaceutical formulations were not demonstrated [13]. There is a necessity to develop a rapid method for the simultaneous analysis of PQ and DHA in combined tablets, especially for the detection of counterfeit or substandard drugs.

Chemometrics-assisted vibration spectroscopic methods (e.g. infrared (IR) and Raman spectroscopy) are gaining popularity for drug analysis due to their

suitability for both identification and quantification. They offer high throughput, minimal sample pretreatment and non-destructive nature. Additionally, they are cost effective and environmentally friendly. Chemometrics-assisted vibration spectroscopy was firstly introduced in 1972 by Svante Wold and Bruce R. Kowalski [14]. Spectroscopic methods mainly associated with the absorption, emission and scattering of visible, ultraviolet or IR electromagnetic radiation. Fourier transform IR measures the vibrations of atoms allowing the determination of analytes functional groups [15,16], whereas Raman spectroscopy is based on light scattering phenomenon causing changes in vibrational, rotation or electronic energy of a molecule [17,18]. Previous studies on near IR with partial least squares regression (PLSR) models were developed for the determination of artesunate and azithromycin in co-formulation of hard gelatin capsule [19] and fix-dose combination of anti-tuberculosis tablets (rifampin, isoniazid, pyrazinamide and ethambutol) [20]. FTIR with PLSR pretreated raw data by first derivative and Savitzky–Golay smoothing followed by mean centring was employed for the quantitative analysis of combined anti-malaria formulations of artesunate and mefloquine [21]. In addition, Raman spectroscopy with principal component regression (PCR) was employed to quantify dipyrone (metamizole) in oral solutions [22].

This study aimed to establish and validate rapid techniques with minimal sample preparation for PQ and DHA analysis using chemometrics-assisted FTIR and Raman spectroscopy. Reverse phase HPLC was also developed and used as a reference method. Results from spectroscopic methods were statistically compared with the HPLC method. The developed methods could serve as routine methods for quality control of pharmaceutical products and for rapid detection of low quality medications.

2. Materials and methods

2.1. Chemicals

PQ tetraphosphate tetrahydrate and DHA were purchased from Xi' an Sgonek Biological Technology Co., Ltd (Xi'an, China). Acetonitrile and methanol (HPLC grade) were obtained from Thomas Baker (Chemicals) Pvt. Ltd. (Mumbai, India). Ammonium dihydrogen phosphate was of analytical grade purchased from Carlo Erba Reagents S.A.S (Barcelona, Spain). Octanesulfonate was from Sigma–Aldrich (St. Louis, Missouri, USA). Combined tablets of PQ (320 mg) and DHA (40 mg) were from local

manufacturers. Placebo obtained from the Government of Pharmaceutical Organization (Bangkok, Thailand) (e.g. pregelatinized starch, hypromellose, croscarmellose sodium, magnesium stearate, dextrin, titanium dioxide and macrogol 400) was prepared by mixing all excipients as indicated in tablet leaflet.

2.2. Standard and sample preparations for HPLC-UV method

Starndard PQ and DHA were accurately weighed and diluted with 50% acetonitrile to concentrations of 265 μg/mL for PQ and 33 μg/mL for DHA. Twenty tablets of the samples were weighed and ground to fine powder. The powder was accurately weighed and diluted with 50% acetonitrile to the same concentrations as the standards. Standard and sample solutions were sonicated for 20 min to ensure complete dissolution. All solutions were freshly prepared, protected from light, and filtered through a 0.22 μm membrane filter before injection in to the optimum HPLC system.

2.3. Development of HPLC-UV method

Chromatographic separation was performed on a on HPLC Dionex Ultimate 3000 and Chromeleon™ chromatography data system software for data acquisition. Column and autosampler temperatures were set at 25 and 10 °C, respectively. Method optimization for the separation of PQ and DHA epimers was achieved by varying column (C8, 4.6 mm, i.d.) lengths (150 and 100 mm) and particle sizes (5 and 3 μm) and mobile phase compositions (10–20 mM ammonium dihydrogen and phosphate (pH 4.5) and 10–20 mM octanesulfonate containing methanol or acetonitrile), The optimum condition was determined from resolution (R_s), tailing factors (TF), numbers of theoretical plates (N) and precision (%RSD). Method validation was evaluated in terms of specificity, linearity, precision and accuracy according to ICH guideline [23].

2.4. Collection of FTIR spectra

A FTIR spectroscopy NicoNicolet™ iS™ 5 FTIR Spectrometer (Thermo fisher scientific, Waltham, USA) and OMNIC spectra software was used throughout the study. Prior the measurements, the tablets were ground to fine powder. The %transmittance was collected from wavenumbers 400–4,000 cm^{-1} using attenuate total reflectance (ATR) mode. Resolution, gain and number of scans were set at 4, 1 and 32, respectively.

2.5. Collection of Raman spectra

Raman spectra were measured by Metrohm handheld Raman spectrometer with Mira P. software using scattering mode. Prior the measurements, the tablets were ground to fine powder. The intensity was collected from wavenumbers 400—2,300 cm^{-1}. Integration time was set at 5.0 s, average was set at 3, laser power was set at 100 mW and wavelength was set at 785 nm.

2.6. PLSR models for PQ and DHA content measurements

Twenty synthetic samples for a calibration set, fifteen synthetic samples for a validation set were prepared according to a central composition design (CCD) [24,25] with three ingredients consisting of PQ and DHA and the excipients. The central point of the CCD corresponds to 320 mg PQ, 40 mg DHA and 190 mg excipients. This setting was used in accordance to the fix dose formulation of PQ and DHA tablets. The ranges of PQ and DHA were varied from 50 to 150% of the middle point content.

All spectra data were collected by FTIR and Raman spectroscopy using the optimum conditions. All spectra data and actual PQ and DHA contents from HPLC-UV method were subjected to the Unscrambler® program for PLSR modelling. The spectroscopic spectra of the samples were pretreated with different methods including Savitzky−Golay first derivatives (Dl), Savitzky−Golay second derivatives (D2) [26,27], baseline correction [27,28], orthogonal signal correction (OSC) [29], standard normal variate (SNV) [30,31] and detrending [27]. The pretreatment is applied prior the model construction in order to simplify the model and data interpretation. Derivatives are the most common signal pretreatments applied to spectral data. Derivatives are mainly used to resolve overlapped peaks (or enhance resolution) and eliminate constant and linear baseline drift between samples. The Savitzky−Golay is the most common derivative method, requires selection of polynomial order (second or third order are normally used) and window size (which must be an odd number higher than the polynomial order) [26,27]. The proper window size depends on the spectral resolution, noise and the amplitude of the absorption(s) band(s) of interest. Noise and baseline are two common problems in analytical chemistry. Both of them lead to the deterioration of accuracy and precision. Baseline correction is an important pre-processing technique that is used to separate true spectroscopic signals from interference effects or to remove background noises, stains or traces of

compounds [27,28]. OSC is a pre-processing technique used for removing the information unrelated to the target variables. It bases on the constrained principal component analysis associated with a processing step that improves the calibration model by removing systematic variation from the response matrix X that is unrelated, or orthogonal, to the property matrix Y. OSC is a suitable pre-processing method for PLSR of mixtures without loss of prediction capacity using spectrophotometric methods [29]. The spectral pretreatments known as (SNV) are designed to remove the multiplicative interferences from reflectance spectra at least some of the large amount of variability that may be caused by scattering effects [30]. In SNV, each spectrum is transformed by subtracting the spectrum mean and dividing by the spectrum standard deviation [31]. De-trending is performed through subtraction of a linear or polynomial fit of baseline from the original spectrum to remove tilted baseline variation, usually found in NIR reflectance spectra of powdered samples and Raman spectra with fluorescence background reference. Each spectrum is adjusted with a first or second order polynomial. Finally, the original spectra are subtracted by adjusted spectrum to obtain the corrected spectrum. Although higher order polynomials may be used, there is an associated risk of removing relevant information [27].

All samples were evaluated using PCR [32,33] to observe the relationships between samples and variables. Then, 105 spectra data were selected as a calibration set to construct models. The remaining 35 spectra data were classified as a validation set for testing the efficiency of the model using Kennard-Stone algorithm [31]. After grouping all synthetic samples into calibration and validation sets, the samples in each pretreatment and the original data was used to construct the calibration models using PLSR algorithm [29,30] and internally validated by cross validation. An appropriate choice of the wavenumbers is necessary for calibration model construction. Thus, PLSR models were constructed from full range spectra comparing with various wavenumbers intervals, which were manually selected by Jackniffing algorithm [34]. The optimal model was evaluated from parameters including determination coefficient (R^2) between the predicted and reference values of the calibration model, which should be more than 0.9, root mean squared error of prediction (RMSEP), relative standard error of prediction (RSEP), bias and p-value [35]. RMSEP is the simplest and the most efficient measure of the uncertainty for predictive ability of multivariate models by comparing predictions with reference values for a validation set (Eq (1)). RSEP is a

common practice to estimate the predictive ability of multivariate models by comparing predicted with reference values for a validation set (Eq (2)). RSEP is a parameter that indicates the uncertainty of a model and is represented as percent.

$$RMSEP = \sqrt{\frac{1}{N}\sum(\widehat{y}_i - y_{I,ref})^2} \qquad \text{Eq(1)}$$

where, N = the size of the validation set
$\widehat{Y}_i$ = the prediction value for sample i
$Y_{i,ref}$ = the reference value for sample i

$$RSEP(\%) = 100 \times \sqrt{\frac{1}{N}\sum\frac{(\widehat{Y}_i - Y_{I,ref})^2}{\sum Y_{I,ref}}} \qquad \text{Eq(2)}$$

where, N = the size of the validation set
$\widehat{Y}_i$ = the prediction value for sample i
$Y_{i,ref}$ = the reference value for sample i
Finally, the calibration models were used for prediction of PQ and DHA concentrations in the validation set and sample tablets in comparison with reference values from HPLC.

2.7. Validation of PLSR models of spectroscopic methods

Validation of the PLSR models of spectroscopic methods was evaluated in terms of specificity, linearity, accuracy and precision. As recommend in ICH Q2 (R2) guideline [23], the loading plots of the PLSR models can be used to confirm specificity of the assay method. In principle, a PLSR model for a certain substance is performed from the model input data with respected to such specific response. Therefore, the loading plot, a plot of model contributed variables, can present the specific characteristics information of the target response. Linearity regression of model was obtained by plotting predicted PQ and DHA concentrations from the determination model (Y) versus PQ and DHA actual concentrations from the HPLC-UV method (X). R^2 should be 0.9 or greater. Method accuracy was accomplished by evaluating the linearity of the relationship between estimated concentrations obtained from the development model and actual concentrations of PQ and DHA obtained from the HPLC method. More than one concentration was used for accuracy experiments since 33 calibration set was employed. The acceptance criteria (at 95% confidence interval) of the slope are around 1.0 indicating the agreement of results from the methods. Precision in term of repeatability was evaluated using six determinations at the middle concentration of the validation set, which represented the real sample (320 mg PQ and

40 mg DHA). Precision was expressed by relative standard deviation (%RSD) and was performed according to ICH Q2 (R2) guideline (Validation of Analytical Procedure), which recommends a minimum of 6 determinations at 100% of the test concentration [23].

2.8. Applications

The developed chemometrics-assisted FTIR and Raman spectroscopy methods were applied to analyze tablets in comparison with the HPLC. Proposed models based on the PLSR was used to determine PQ and DHA in tablets using the optimum wavenumbers and latent factors. Results obtained from each method were statistically compared using t-test at 95% confidence intervals. The data were analyzed using Excel®.

3. Results

3.1. Development of HPLC-UV method

In this study, two columns with different lengths and particle sizes were tested and results showed that better peak shapes and separation of PQ and DHA epimers were obtained from C8 column (100 mm × 4.6 mm i.d., 3 μm particle) using a flow rate of 1.0 mL/min. Buffer (20 mM ammonium dihydrogen phosphate (pH 4.5) containing methanol or acetonitrile as organic solvent were studied for the separation of the investigated analytes. Results revealed that acetonitrile offered more symmetric peaks than methanol and it mixed well with the buffer at 50% v/v. Whereas, octanesulfonate buffer (pH 4.5) showed more interference peaks than ammonium dihydrogen phosphate buffer and it was excluded from the study. The suitable wavelengths were 325 nm for PQ and 210 nm for DHA and the retention times were 1.3, 3.3 and 4.6 min for PQ and DHA epimers, respectively (Supplement I). System suitability test under the optimum condition showed R_s of more than 7.7 (calculated from DHA epimers), TF of less than 1.5, N of greater than 2,000 and %RSD of less than 2.0%.

3.2. Method validation of HPLC-UV method

Specificity of the method was done by injecting the diluting and matrix solutions (see 2.1 Chemicals) in comparison with standard solutions of PQ and DHA. Results showed that no interference was observed at the same time of PQ and DHA peaks. Linearity of the method revealed regression of y = 70.444x — 0.6727 (R^2 = 0.9997) in the range of

0.13—0.40 mg/mL for PQ and y = 3.5761x — 0.0042 (R^2 = 0.9994) in the range of 0.016—0.049 mg/mL for DHA. The calibration curve of DHA in HPLC method was established from the sum areas of α- and β-DHA since both forms slowly equilibrate. Accuracy of the method was represented as %recovery from standard addition experiments with 3 concentrations covering the range of 50—150% of the labelled amounts. The mean recoveries of PQ and DHA were 99.9 and 99.1%, respectively. Repeatability was expressed as the %RSD of six samples. Results showed %RSD of intra-day for PQ and DHA were of 0.63% and 0.39%, respectively and %RSD of inter-day of PQ and DHA were 0.88% and 0.88%, respectively.

3.3. PLSR models for PQ and DHA content measurements

Initially, the combined tablets of PQ and DHA were directly measured using FTIR and Raman spectroscopy. However, the principal bands of PQ and DHA from both methods could not be observed. Thus, chemometric-assisted techniques using PLSR were applied to achieve the accurate quantitation of PQ and DHA in the tablets.

FTIR spectra from 35 synthetic samples (105 spectra) and 23 samples of tablets were directly measured. Relationships between samples and variables in all synthetic samples were evaluated using PCA. Then, Kennard-Stone algorithm was used to select 70 spectra as the calibration set and 33 spectra from 35 spectra (exclude outlier from error of measurement) was fixed as the validation set. Different data pretreatments were applied to the original data to establish various PLSR models (Supplementary II and III). As shown in Table 1, the optimum model for FTIR spectra of PQ was the model constructed from FTIR spectra pretreated with OSC from spectral interval 400—1,800 cm^{-1} with 9 latent factor (Supplementary IV (A)). The optimum model for FTIR spectra of DHA was the model constructed from FTIR spectra pretreated with OSC from spectra

interval 400—4,000 cm^{-1} with 3 latent factors (Supplementary IV (B)) and 1,400—4,000 cm^{-1} with 7 latent factors (Supplementary IV (C)).

Raman spectra (n = 105) of synthetic samples and the combined tablet powder with their actual PQ and DHA concentrations from HPLC method were subjected to the Unscrambler® software. Then, Kennard-Stone algorithm was used to select 70 spectra as the calibration set and 32 spectra from 35 spectra (exclude outlier from error of measurement) was fixed as the validation set. Different data pretreatments were applied to the original data to establish various PLSR models (Supplementary V and VI). As shown in Table 2, For PQ, the optimum calibration model was from SNV pretreatment. The R^2 of the optimum calibration from wavenumbers 1,200—2,300, cm^{-1} with 6 latent factors was 0.9630 (cross validation = 0.8872) (Supplementary VII (A)), while the R^2 of 32 samples in the validation set plots between predicted values and reference values was 0.9311. Then, the model was used to predict value of the samples comparing with HPLC method since it showed the p-value of more than 0.05. The optimum model for handheld-Raman spectra of DHA was the model constructed from handheld-Raman spectra pretreated with OSC from all selected wavenumbers ranges with 1 latent factor (Supplementary VII (B)).

Figs. 2 and 3 compare the score plots of the original and pretreated data of PQ and DHA from FTIR and Raman measurements. For unpretreated data, it was difficult to differentiate among low, middle and high concentrations of the analytes. It is obvious that the pretreated data showed the improvement in grouping of various concentrations of the analytes. Although some of medium and high concentration samples were still overlapped, the pretreated data showed the improvement in grouping of various concentrations of the analytes compared with unpretreated data. Due to improvement of data arrangement, the PLSR models obtained from pretreated data were superior more than the models constructed from unpretreated data. The optimal model from FTIR spectroscopy for PQ was from

Table 1. Calibration and validation sets of PQ and DHA contents by PLSR models from FTIR spectroscopy.

Drug	Data Pretreatment[a]	Latent factors	Calibration set			Validation set			Sample
			Wavenumber (cm^{-1})	R^2 (model)	R^2 (cross validation)	R^2 (Pearson) Prediction	Bias	RSEP	p-value
PQ	OSC	8	400—4,000	0.9816	0.9216	0.9234	4.08	10.40	0.8626
		9	400—1,800	0.9775	0.9026	0.9512	7.34	8.75	0.6122
		5	1,400—4,000	0.9680	0.9285	0.9027	2.10	11.64	0.6667
DHA	OSC	3	400—4,000	0.9004	0.8510	0.9018	0.82	13.63	0.1016
		7	1,400—4,000	0.9644	0.8535	0.9305	1.88	11.79	0.2309

[a] OSC = Orthogonal signal correction.

Table 2. *Calibration and validation sets of PQ and DHA contents by PLSR models from Raman spectroscopy.*

Drug	Data pretreatment[a]	Latent factors	Calibration set			Validation set			Sample
			Wavenumber (cm^{-1})	R^2 (model)	R^2 (cross validation)	R^2 (Pearson) Prediction	Bias	RSEP	p-value
PQ	SNV	6	1,200−2,300	0.9630	0.8872	0.9311	6.87	8.81	0.1114
DHA	OSC	1	400−2,300	0.9455	0.9432	0.9778	0.35	7.97	0.5665
		1	1,200−2,300	0.9455	0.9450	0.9778	0.36	7.97	0.5649
		1	400−1,400	0.9456	0.9443	0.9778	0.35	7.97	0.5658

[a] SVN = Standard normal variate, OSC = Orthogonal signal correction.

OSC pretreatment at wavenumbers 400−1,800 cm^{-1} and for DHA was from OSC pretreatment at wavenumbers 1,400−4,000 cm^{-1}. For Raman spectroscopy, the optimum model of PQ was from SNV pretreatment at wavenumbers 1,200−2,300 cm^{-1} and DHA was from OSC pretreatment at wavenumbers 400−2,300 cm^{-1}. The optimum wavenumber ranges for both analytes were assessed from the highest correlation between actual and predicted values obtained from calibration step (R^2 model and R^2 of cross-validation) and test set prediction step (R^2 Pearson) and the lowest error parameters such as bias and RSEP are criteria for selection the most suitable models.

Figs. 4 and 5 represent the overlaid FTIR and Raman spectra, respectively, obtained from the combined tablet powder and standard PQ and DHA. The characteristic IR peaks are corresponded to the functional groups of PQ and DHA including the broad band of −OH stretching at 3,200−3,300 cm^{-1},
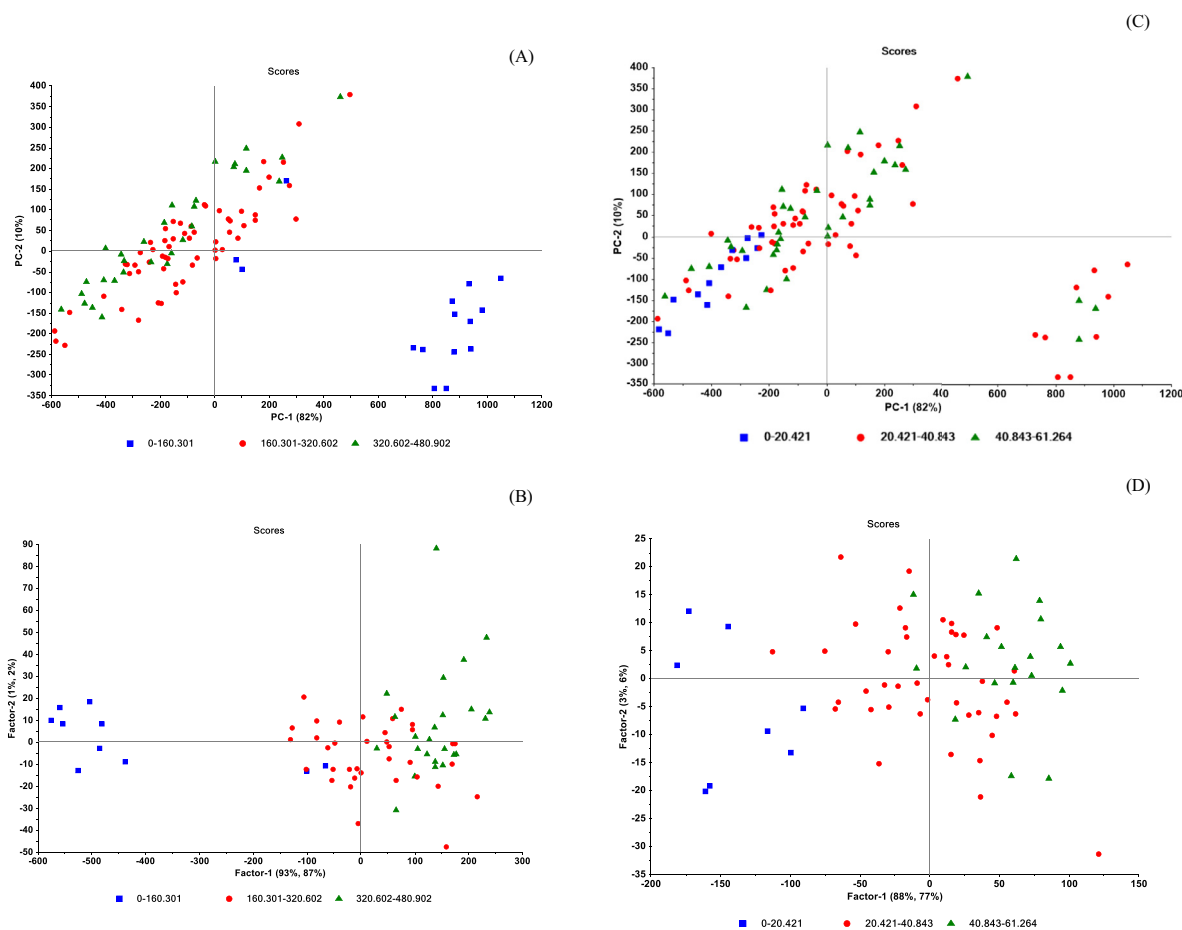

Fig. 2. *Score plots of (A) unpretreated FTIR spectral data of PQ, (B) pretreated FTIR spectral data of PQ, (C) unpretreated FTIR spectral data of DHA and (D) pretreated FTIR spectral data of DHA at low, middle and high concentrations.*
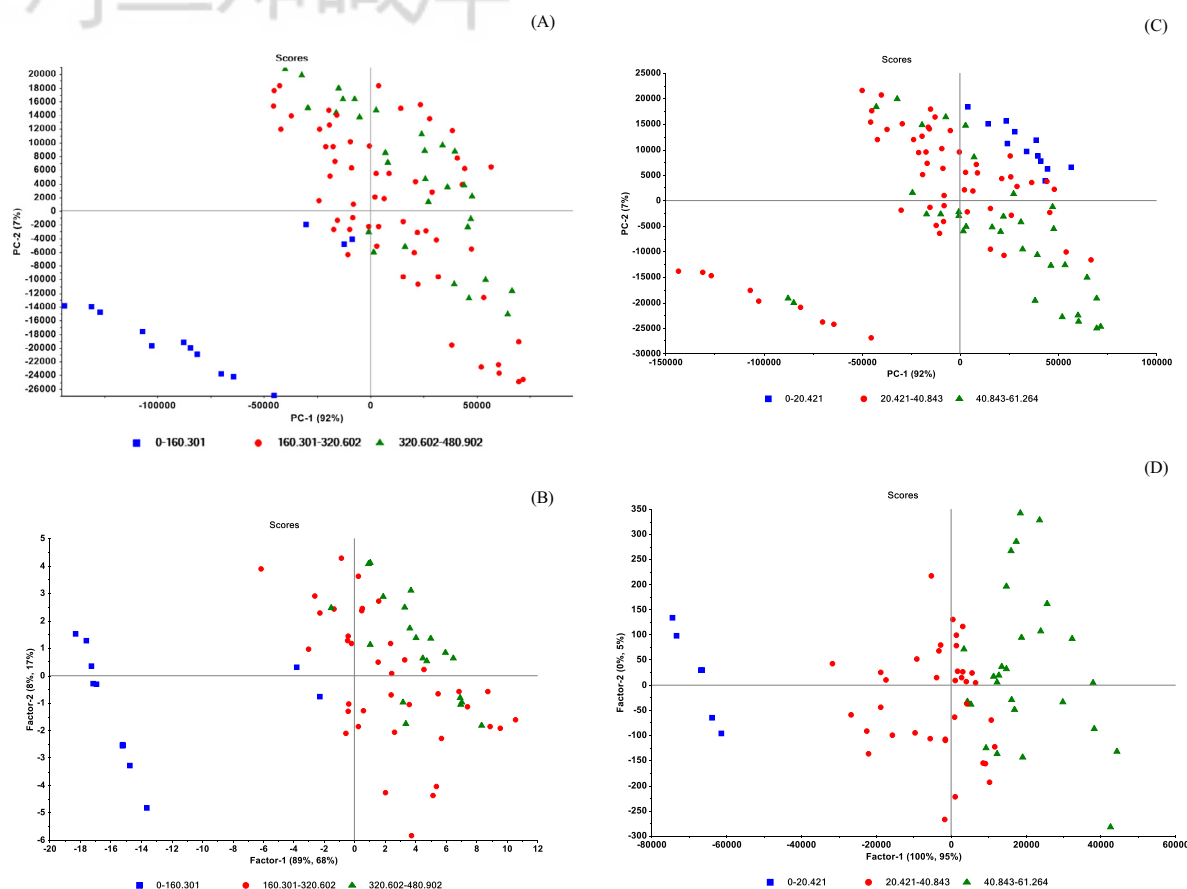
Fig. 3. *Score plots of (A) unpretreated Raman spectral data of PQ, (B) pretreated Raman spectral data of PQ, (C) unpretreated Raman spectral data of DHA and (D) pretreated Raman spectral data of DHA at low, middle and high concentrations.*

C−C stretching in ring at 1,400−1,650 cm^{-1}, aromatic C=C bending at 1,500−1,700 cm^{-1} and C−H stretching at 2,900−3,300 cm^{-1} (49, 50). The characteristic Raman peaks are corresponded to the structure of PQ and DHA including the broad band of CH$_2$ at 1,449 cm^{-1}, C−O−C at 1,060−1,150 cm^{-1} and C−C at 600−1,300 cm^{-1} for DHA. For PQ, strong peak at 1,382 cm^{-1} and 1,594 cm^{-1} corresponded to CH$_2$ bending or twisting and aromatic ring chain vibration, respectively (51).

3.4. Validation of PLSR models of spectroscopic methods

Validation of the PLSR models for the quantitation of PQ and DHA in the combined tablets were determined from analytical performance characteristics including specificity, linearity, accuracy and precision. Method specificity was evaluated from loading plot of the PLSR models [23]. The loading plots of the models from FTIR and Raman spectral data of PQ and DHA shows the principle bands

those corresponding to the functional groups present in the structure of PQ and DHA, which are highly specific [Supplement VIII-XI]. The linear regression of PLSR models from optimal models was obtained by plotting prediction values of PQ and DHA from the validation set and the actual concentrations from HPLC method. The R^2 of the optimum PLSR model of PQ and DHA from FTIR spectra with OSC pretreatment method were 0.9512 and 0.9305, respectively (Fig. 6(A)−(B)). The R^2 of the optimum PLSR model of PQ and DHA from Raman spectra were 0.9311 (SNV pretreatment) and 0.9778 (OSC pretreatment), respectively (Fig. 7(A)−(B)). These values indicated the strong correlation of the methods with high R^2 values of greater than 0.9305. Agreement between FTIR, Raman and HPLC for quantitative determination of PQ and DHA were illustrated by Bland−Altman plots in Fig. 6(C)−(D)) and 7 (C)-(D)). The plots show random variability of data points and the majority of the data points locate within ±2SD of the mean difference [36,37]. Although the positive bias was found from FTIR for PQ, Raman for PQ and
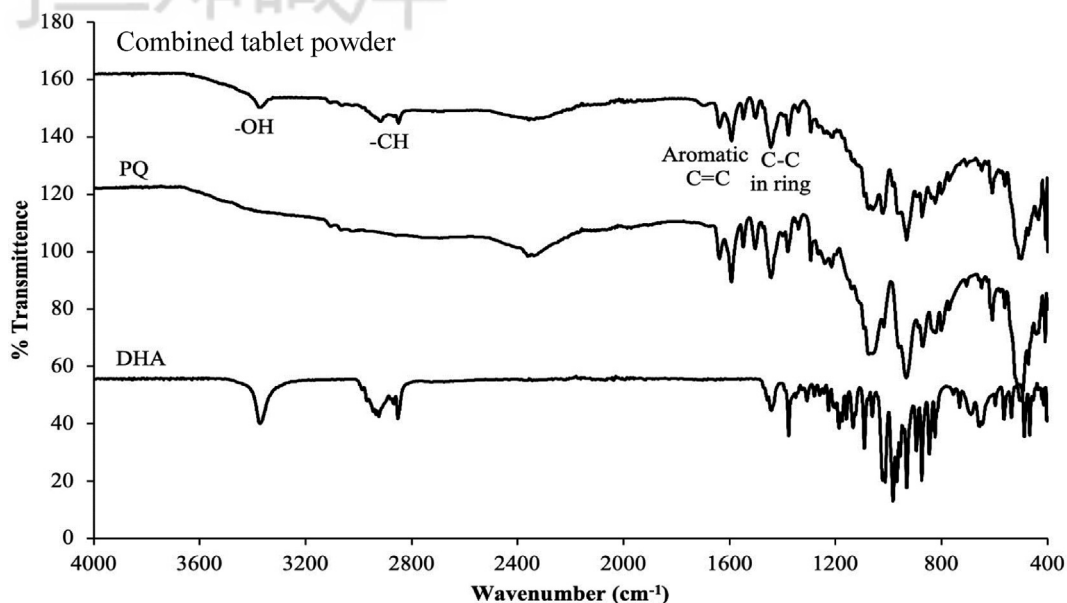
Fig. 4. Overlaid FTIF spectra of combined tablet powder and standard PQ and DHA.

DHA, these bias values were not significant, because the lines of equality were with the confidence interval of the mean difference (Table 4). For DHA, positive bias of FTIR determination method compared with HPLC was found significant. However, this was acceptable due to the close of upper confidence interval and the line of equality (−0.21 vs. 0.0). Method accuracy was evaluated by comparing slopes of the regression from the optimum PLSR models and from HPLC-UV method. Results show the slopes and their confidence interval (at 95%) around 1.0 reavealing

the agreement of the proposed and reference methods. Precision represented as %RSD (n = 6) and %RSEP (n = 33) were within 4.1−10.6 and 7.97−11.79%, respectively. Thus, specificity, linearity, accuracy and precision of the developed methods are in acceptable range.

3.5. Applications

The developed chemometrics-assisted FTIR and Raman spectroscopic methods were applied to
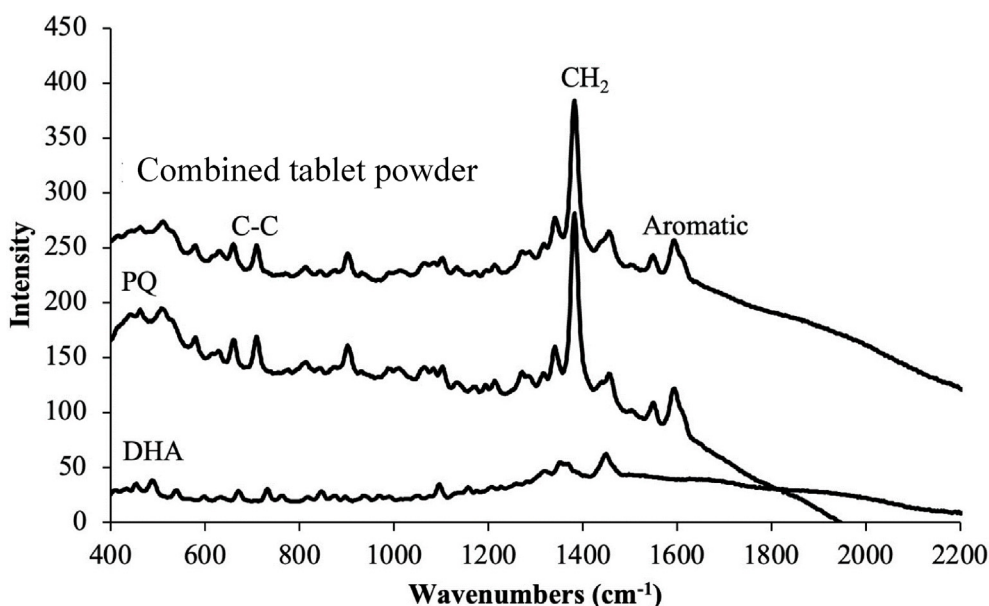

Fig. 5. Overlaid Raman spectra of combined tablet powder and standard PQ and DHA.
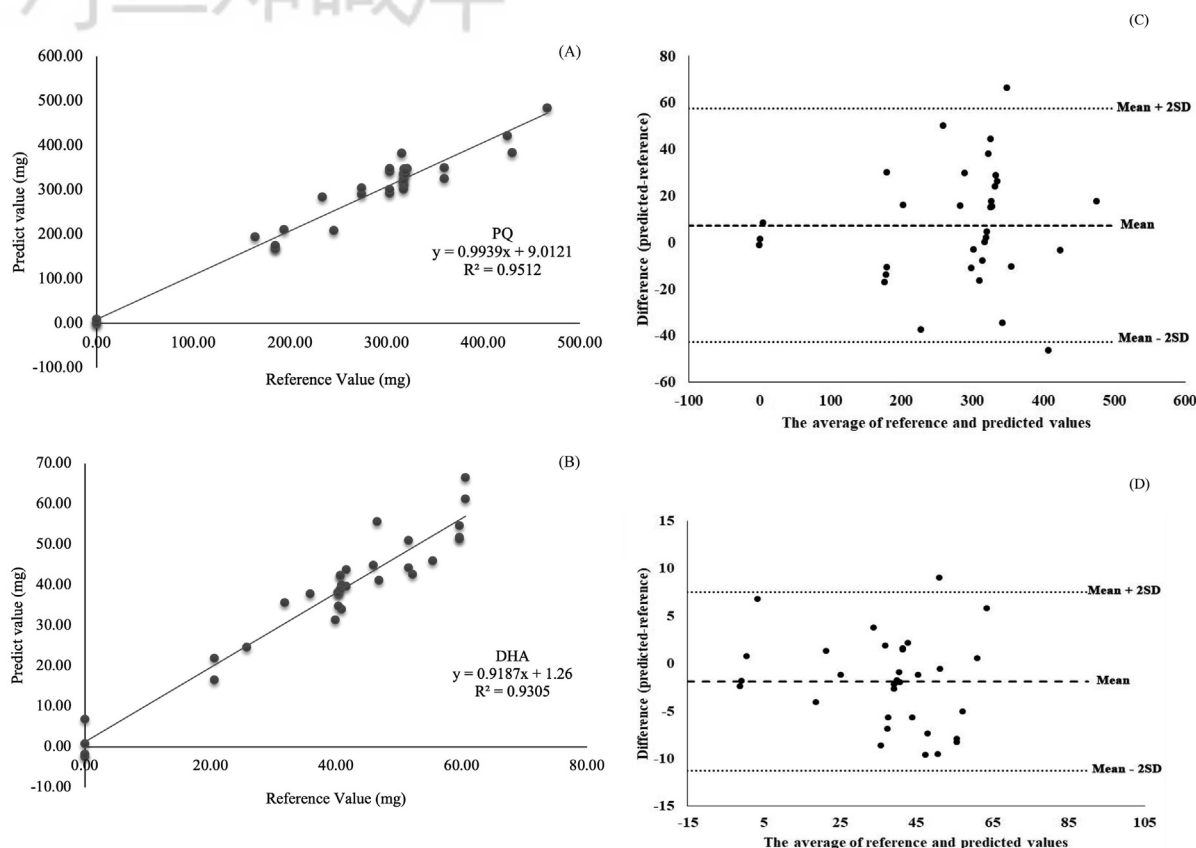
Fig. 6. Linearity curves between predicted concentrations and reference values from FTIR spectroscopy of (A) PQ (400—1,800 cm^{-1}) with OSC pretreatment and (B) DHA (1,400—4,000 cm^{-1}) with OSC pretreatment. Bland Altman plots of predicted concentrations and reference values from FTIR spectroscopy of (C) PQ (400—1,800 cm^{-1}) with OSC pretreatment and (D) DHA (1,400—4,000 cm^{-1}) with OSC pretreatment.

analyze the samples in comparison with the HPLC-UV method (Table 3). Result from FTIR spectroscopy showed the average amount of 352.45 mg (% RSD = 7.00, n = 23) PQ and 45.87 mg DHA (% RSD = 14.1, n = 23). For Raman spectroscopy, the average amounts of PQ and DHA from the optimal models were 363.60 mg (%RSD = 11.7, n = 25) and 44.51 mg (%RSD = 5.2, n = 25), respectively. The larger RSD and RE from the spectroscopic methods might stem from the homogeneity of the sample. In HPLC, samples were injected as solution, which were homogeneous. Whereas, they were analyzed as powder in spectroscopic methods.

Results obtained from each method were compared with HPLC-UV method using t-test at the 95% confidence intervals. The results were not significantly different at 95% confidence limit (p-value >0.05). Thus far, there is no monograph of combined tablet of PQ and DHA available in any pharmacopeia. The labeled amounts of all methods were about 110.0%, which were within limits of most drug products in pharmacopeia (90.0−110.0%).

4. Discussion

Chemometrics-assisted spectroscopic methods were successfully developed for the rapid determination of PQ and DHA in tablets. PLSR models were constructed by using data from FTIR and Raman spectroscopy in the calibration and validation sets.

Firstly, the HPLC method was developed by optimizing factors including stationary phase, mobile phase and detecting wavelengths. The optimal HPLC method was achieved on an Inertsil® column (C8, 100 mm × 4.6 mm, 3 μm) with a flow rate of 1.0 mL/min, using an isocratic system of 20 mM ammonium dihydrogen phosphate and acetonitrile (50:50) as the mobile phase with detection wavelengths at 325 nm and 210 nm for PQ and DHA, respectively. The optimal condition provided a baseline separation of all analytes and no interference at the same retention time of PQ and DHA peaks. Run time of method was 6 min with good system suitability. The HPLC condition was validated in terms of specificity, linearity, accuracy and precision. The linearity (R^2 > 0.999) accuracy
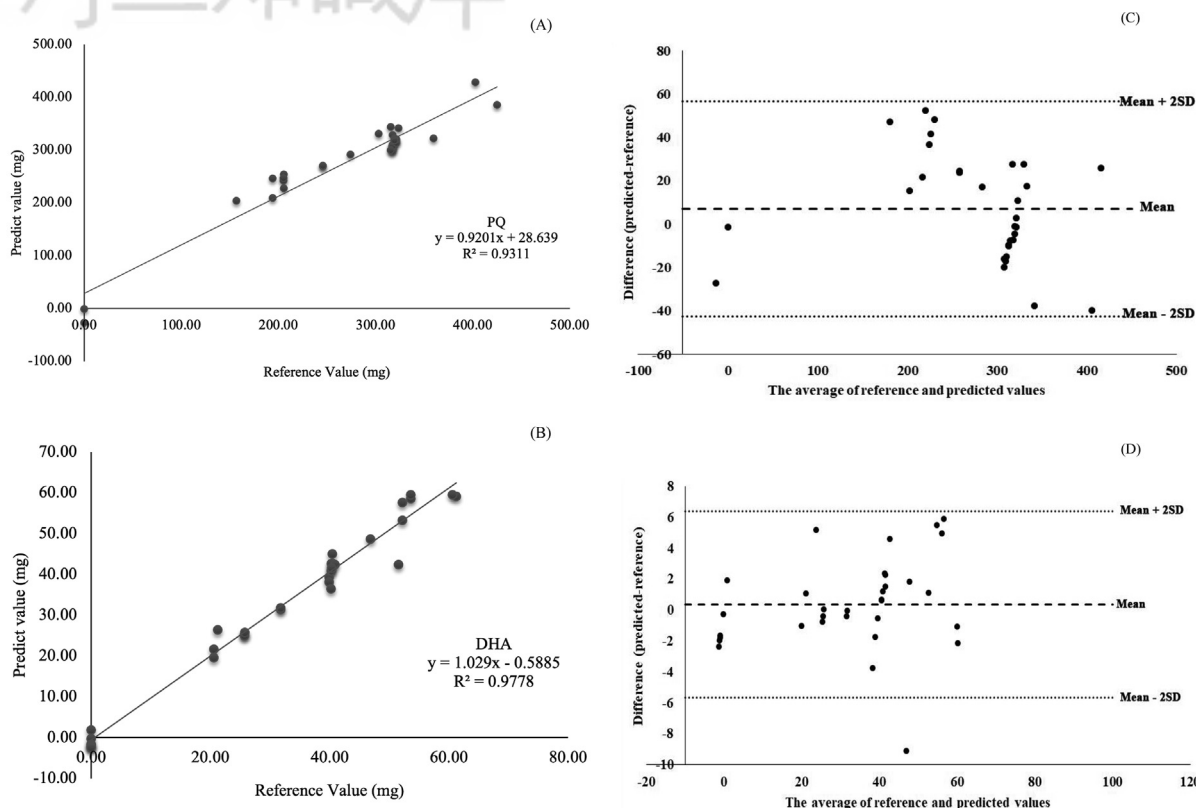
Fig. 7. Linearity curves between predicted concentrations and reference values from Raman spectroscopy of (A) PQ (1,200—2,300 cm^{-1}) with SNV pretreatment and (B) DHA (400—2,300 cm^{-1}) with OSC pretreatment. Bland Altman plots of predicted concentrations and reference values from Raman spectroscopy of (C) PQ (1,200—2,300 cm^{-1}) with SNV pretreatment and (D) DHA (400—2,300 cm^{-1}) with OSC pretreatment.

represented as %recovery (99.5%, %RSD <1.5% (n = 9)) and precision (%RSD <0.88%, n = 6) were acceptable. Validation data of the HPLC-UV method show that the method is valid and suitable to be used as a reference method for this work.

PQ and DHA contents in the combined tablets were determined using several PLSR models based on the original and pretreated FTIR and Raman spectra with reference values from the optimized HPLC method. The large different ratio of PQ and DHA (320 versus 40 mg) in the combined tablets was a main challenge of this work. In addition, IR absorption bands with mild and moderate intensities obtained from single bonds functional groups in DHA structure was another challenge for development of PLSR model for

DHA from IR spectral data. Generally, spectroscopic methods might be suffered from instrumental noises light scattering and baseline shifts [35]. Due to these drawbacks, poor precision and inappropriate calibration modeling are usually obtained from original spectroscopic spectra. To overcome the problems, original spectra from spectroscopic methods are usually pretreated with different pretreatment methods (e.g. SNV, OSC, D1 and D2) to improve the calibration model performance, to suppress noises and baseline shifts.

For chemometrics-assisted FTIR and Raman spectroscopy, all 105 spectra were collected and subjected to the Unscrambler® software to construct PLSR model for the determination of PQ and DHA.

Table 3. Assay of the combined tablet using the proposed spectroscopic methods in comparison with the HPLC-UV method.

	Drug[a]	Label claimed (mg)	Spectroscopy (mg)	HPLC (mg)	p-value
FTIR	PQ	320	352.45 ± 24.65	349.81 ± 0.99	0.61
	DHA	40	45.87 ± 6.46	44.24 ± 0.02	0.23
Raman	PQ	320	363.60 ± 42.49	349.81 ± 0.99	0.11
	DHA	40	44.51 ± 2.33	44.24 ± 0.02	0.57

[a] PQ = Piperaquine, DHA = Dihydroartemisinin.

Table 4. The elements to calculate confidence intervals of difference mean of Bland−Altman plots.

Method	Difference mean	Standard deviation	Standard error formula	Standard error (se)	t value (32 degree of freedom)	Confidence (se*t)	Confidence intervals	
							From	To
FTIR (PQ)	7.34	25.05	$\sqrt{SD^2/n}$	4.36	2.04	8.90	−1.56	16.24
FTIR (DHA)	−1.88	4.70	$\sqrt{SD^2/n}$	0.82	2.04	1.67	−3.55	−0.21
Raman (PQ)	6.88	24.81	$\sqrt{SD^2/n}$	4.39	2.04	8.95	−2.07	15.83
Raman (DHA)	0.35	3.02	$\sqrt{SD^2/n}$	0.53	2.04	1.09	−0.74	1.44

Kennard-Stone algorithm were used to select 70 sample spectra as the calibration set and 35 sample spectra were selected as the validation set. The parameters in PLSR modeling including number of latent factors, R^2, RMSEC of model and prediction, RMSEP and bias were investigated. The original data and pretreated data using Dl, D2, baseline correction, OSC, SNV and detrending were investigated by varying the spectra range 400−4,000 cm^{-1}, 400−1,800 cm^{-1}, 1,400−4,000 cm^{-1} for FTIR and 400−2,300 cm^{-1}, 1,200−2,300 cm^{-1}, 400−1,400 cm^{-1} for Raman spectroscopy. All PLSR models were validated and compared with HPLC. The optimum PLSR model of PQ and DHA from FTIR spectroscopy was achieved in pretreated data using OSC at the wavenumbers 400−1,800 cm^{-1} using the latent factor of 9 and at the wavenumbers 1,400−4,000 cm^{-1} using the latent factor of 7, respectively. For Raman spectroscopy of PQ and DHA, the optimal PLSR model was achieved in pretreated data using SNV at the wavenumber 1,200−2,300 cm^{-1} using the latent factor of 6 and pretreated data using OSC at the wavenumber 400−2,300 cm^{-1} using the latent factor of 1, respectively. Validation of the spectroscopic methods, in terms of linearity, accuracy and precision, reveal acceptable value indicating that the methods were appropriate for assays of PQ and DHA in the combined tablet.

Comparing to the HPLC-UV method, the optimal chemometrics-assisted FTIR and Raman spectroscopy were not significantly different (p-value >0.05). The developed chemometrics-assisted spectroscopic methods did not require any sample preparation/ pretreatment prior to the analysis. The methods are rapid (1−3 min), non-destructive and simple without requirement of high skillful operators. Additionally, they are eco-friendly since no organic solvent is required and the uses of other chemicals are minimal. Moreover, handheld Raman spectrometer can be employed as onsite analysis at the port of entry without sample transportation and with low maintenance cost. A main drawback of the spectroscopic methods (%RSDs <10.5%) is the precision, which is less than HPLC method (%RSDs <0.9%). HPLC is a well-known advanced technique with high sensitivity, precision and accuracy. HPLC requires experts for operation, laborious sample preparation and consumption of organic solvent. Results from this work show that HPLC provide better precision and accuracy than FTIR and Raman spectroscopy. However, validation data of the two latter methods are in acceptable ranges. Both of FTIR and Raman spectroscopy can serve as reasonable alternatives for quantification of PQ and DHA in combined formulations, especially in resources limited areas.

5. Conclusion

This work presents rapid and non-destructive spectroscopic methods for the simultaneous determination of PQ and DHA in combined formulations. A simple reverse phase HPLC was also developed as reference method comparing with the chemometrics-assisted IR and Raman spectroscopy. Both spectroscopic methods can serve as reasonable alternatives for quantification of combined tablets, which offer significant advantages over conventional method in term of simplicity, speed, cost-effectiveness and environmental friendliness. Furthermore, Raman spectroscopy can serve as a portable device for onsite analysis to deter the importation of counterfeit and substandard drugs to Thailand.
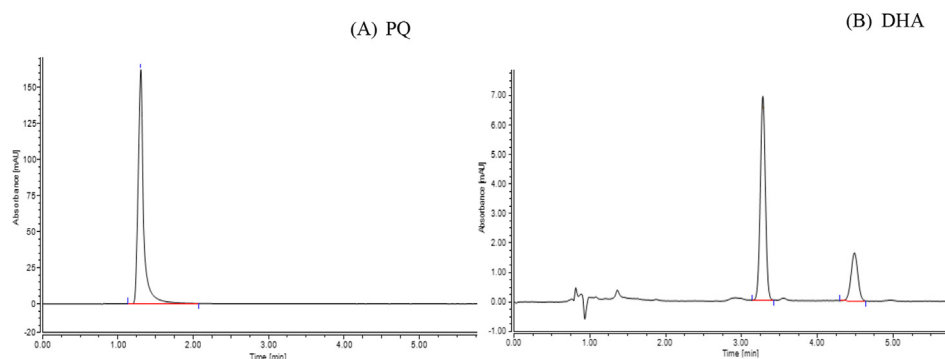
Conflict of interest

The authors declare that there is no conflict of interests.

Appendix

(A) PQ　　　　　　　　　　　　(B) DHA

Supplementary I. The representative chromatogram of the optimum condition of (a) PQ and (b) DHA: HPLC column is C8, 4.6 mm × 100 mm, 3 μm, flow rate 1 mL/min, mobile phase is acetonitrile: 20 mM ammonium dihydrogen phosphate (50:50) detect at UV 325 nm for PQ and 210 nm for DHA.

Supplementary II. Calibration and validation sets of PQ contents by PLSR models from FTIR spectra.

Data Pretreatment	Latent factors	Calibration set				Validation set			Sample
		Wavenumber (cm^{-1})	R^2 (model)	R^2 (cross validation)	R^2 (Pearson) Prediction	Bias	RSEP	RMSEP	p-value
No	5	400−4,000	0.9069	0.8613	0.8752	-4.47	13.67	40.22	7.09E^{-18}
	6	400−1,800	0.9183	0.8481	0.9055	-1.94	11.56	34.00	3.26E^{-12}
	9	1,400−4,000	0.9788	0.9340	0.9023	-3.91	12.23	36.00	5.36E^{-16}
D1	10	400−4,000	0.9494	0.7275	0.8161	5.61	15.23	44.82	0.2861
	8	400−1,800	0.9110	0.6567	0.8148	9.68	16.35	48.13	0.4463
	3	1,400−4,000	0.9442	0.8057	0.8412	9.31	16.37	48.15	0.9016
D2	9	400−4,000	0.9165	0.4375	0.8292	6.50	15.87	46.70	4.07E^{-06}
	9	400−1,800	0.8969	0.2749	0.8286	7.14	15.94	46.91	1.25E^{-06}
	3	1,400−4,000	0.9209	0.7768	0.8289	13.00	16.27	47.87	1.14E^{-08}
Baseline	10	400−4,000	0.9646	0.8877	0.8830	1.15	12.74	37.48	1.72E^{-17}
	10	400−1,800	0.9583	0.8522	0.9188	5.50	10.77	31.70	6.32E^{-26}
	9	1,400−4,000	0.9751	0.9331	0.9084	6.64	11.92	35.08	4.38E^{-15}
OSC	**8**	**400−4,000**	**0.9816**	**0.9216**	**0.9234**	**4.08**	**10.40**	**30.59**	**0.8626**
	9	**400−1,800**	**0.9775**	**0.9026**	**0.9512**	**7.34**	**8.75**	**25.74**	**0.6122**
	5	**1,400−4,000**	**0.9680**	**0.9285**	**0.9027**	**2.10**	**11.64**	**34.24**	**0.6667**
SNV	4	400−4,000	0.9626	0.9451	0.9221	-3.56	10.75	31.64	7.03E^{-20}
	4	400−1,800	0.9534	0.9136	0.9311	-0.09	9.77	28.74	1.32E^{-15}
	5	1,400−4,000	0.9647	0.9557	0.8959	-4.80	1.66	38.24	3.39E^{-25}
Detrending	4	400−4,000	0.9752	0.8650	0.9215	4.40	10.57	31.10	4.40E^{-26}
	2	400−1,800	0.9633	0.8423	0.9225	6.70	10.61	31.23	1.10E^{-25}
	8	1,400−4,000	0.9736	0.9113	0.8946	-4.75	12.70	37.37	9.88E^{-15}

Supplementary III. The calibration and validation sets of DHA contents by PLSR models from FTIR spectra.

Data Pretreatment	Latent factors	Calibration set				Validation set			Sample
		Wavenumber (cm^{-1})	R^2 (model)	R^2 (cross validation)	R^2 (Pearson) Prediction	Bias	RSEP	RMSEP	p-value
No	8	400−4,000	0.9376	0.8850	0.9170	-1.37	13.31	5.64	7.43E^{-12}
	7	400−1,800	0.9178	0.8294	0.8950	-1.80	15.20	6.45	2.78E^{-07}
	8	1,400−4,000	0.9513	0.8552	0.9250	-2.23	12.81	5.43	1.20E^{-18}
D1	8	400−4,000	0.9310	0.7406	0.8768	-2.34	18.39	7.80	0.0158
	9	400−1,800	0.9337	0.7315	0.8851	-2.41	17.25	7.31	0.0288
	6	1,400−4,000	0.9890	0.6147	0.7905	-2.38	23.24	9.86	9.26E^{-08}
D2	1	400−4,000	0.0307	0.0143	0.0071	-3.86	42.24	17.91	1.09E^{-15}
	1	400−1,800	0.0307	0.0125	0.0072	-3.86	42.24	17.91	9.26E^{-08}
	1	1,400−4,000	0.3606	0.0543	0.2130	-1.92	37.23	15.78	4.44E^{-08}
Baseline	9	400−4,000	0.9409	0.8824	0.9191	-1.07	12.97	5.50	3.66E^{-12}
	8	400−1,800	0.9295	0.8730	0.9027	-1.06	14.17	6.01	4.95E^{-11}
	7	1,400−4,000	0.9243	0.8708	0.9079	-2.24	13.79	5.85	4.27E^{-15}
OSC	**3**	**400−4,000**	**0.9004**	**0.8510**	**0.9018**	**-0.82**	**13.63**	**5.78**	**0.1016**
	4	400−1,800	0.9024	0.8105	0.9133	-0.61	13.21	5.60	0.0430
	7	**1,400−4,000**	**0.9644**	**0.8535**	**0.9305**	**-1.88**	**11.79**	**5.00**	**0.2309**
SNV	7	400−4,000	0.9346	0.8836	0.8806	-1.43	14.86	6.30	4.29E^{-19}
	6	400−1,800	0.9119	0.8519	0.9457	-0.89	10.86	4.60	5.92E^{-17}
	6	1,400−4,000	0.9289	0.8697	0.8998	-2.61	14.84	6.29	7.46E^{-29}
Detrend	7	400−4,000	0.9401	0.8873	0.9152	-1.20	13.33	5.65	2.52E^{-13}
	7	400−1,800	0.9299	0.8637	0.8991	-1.07	14.07	5.97	4.13E^{-11}
	9	1,400−4,000	0.9808	0.9004	0.9084	-2.84	14.74	6.25	2.00E^{-21}

(A)

(B)

(C)
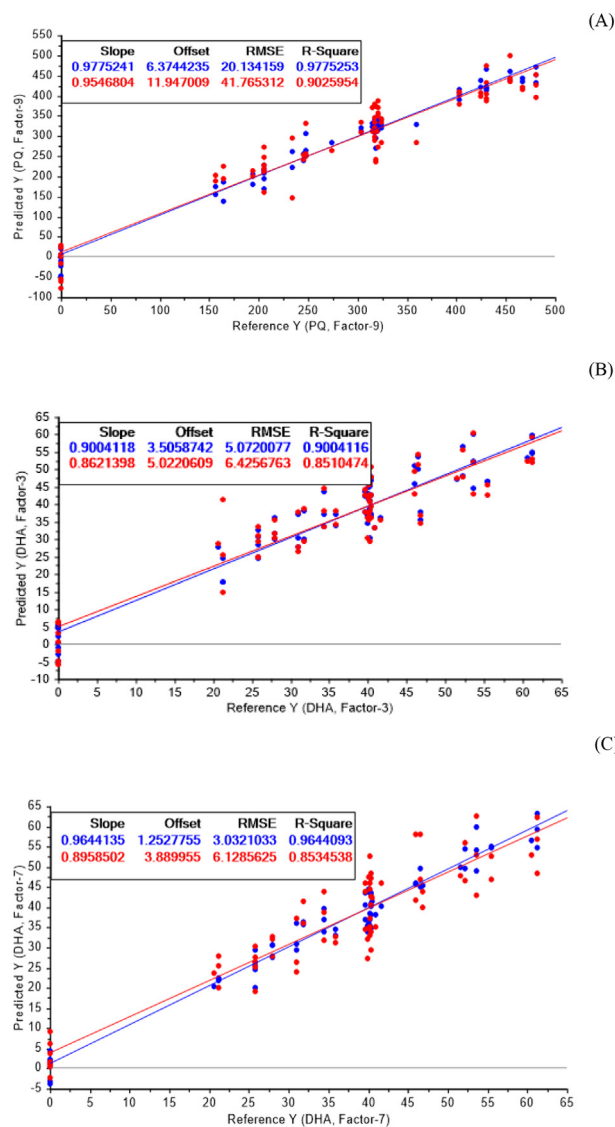
Supplement IV. Calibration curves of PLSR model (blue) and cross validation (red) of (A) PQ from FTIR spectra (400—1,800 cm^{-1}) with OSC pretreatment, (B) DHA from FTIR spectra (400—4,000 cm^{-1}) with OSC pretreatment and (C) DHA from FTIR spectra (1,400—4,000 cm^{-1}) with OSC pretreatment.
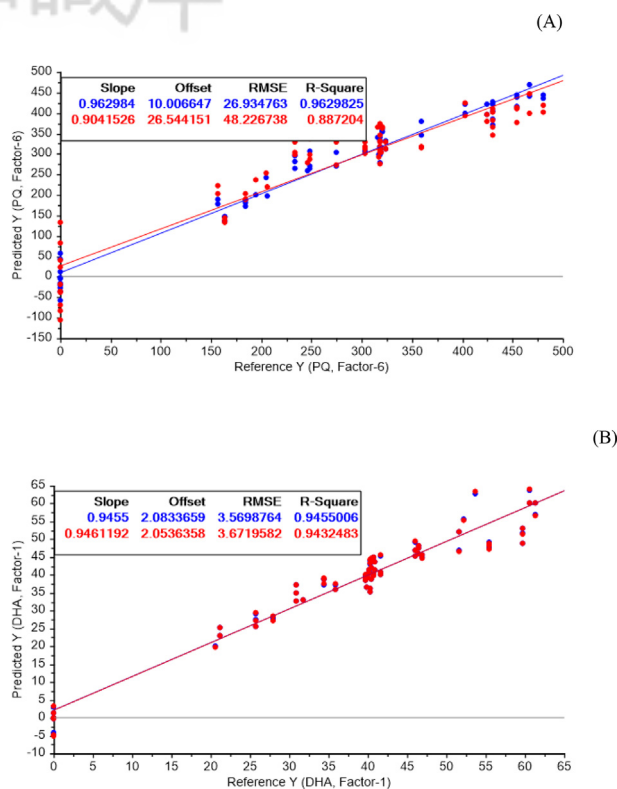
*Supplementary V. Calibration and validation sets of PQ contents by PLSR models from handheld-Raman spectra.*

Data Pretreatment	Latent factors	Calibration set				Validation set			Sample
		Wavenumber (cm^{-1})	R^2 (model)	R^2 (cross validation)	R^2 (Pearson) Prediction	Bias	RSEP	RMSEP	p-value
No	8	400−2,300	0.9706	0.8744	0.8128	6.36	14.18	40.82	3.96E^{-21}
	6	1,200−2,300	0.9287	0.8395	0.8053	1.54	14.33	41.27	4.41E^{-25}
	6	400−1,400	0.8888	0.7826	0.8652	13.30	12.73	36.64	6.53E^{-22}
D1	2	400−2,300	0.9610	0.8107	0.8284	20.60	15.23	43.86	4.18E^{-21}
	2	1,200−2,300	0.9598	0.8089	0.8038	23.16	16.85	48.51	9.76E^{-24}
	2	400−1,400	0.9007	0.7380	0.8270	20.10	15.14	43.58	1.90 E^{-16}
D2	2	400−2,300	0.9318	0.7947	0.7788	19.48	17.31	49.84	4.07E^{-22}
	2	1,200−2,300	0.9269	0.8037	0.7703	19.58	17.66	50.86	9.46E^{-26}
	1	400−1,400	0.8119	0.8049	0.7259	23.46	16.90	48.67	3.51E^{-39}
Baseline	8	400−2,300	0.9706	0.8631	0.8129	6.36	14.18	40.82	3.96E^{-21}
	6	1,200−2,300	0.9287	0.8707	0.8053	1.54	14.33	41.27	4.41E^{-25}
	6	400−1,400	0.8888	0.8064	0.8652	13.36	12.73	36.64	6.53E^{-22}
OSC	2	400−2,300	0.9854	0.9237	0.8572	8.90	12.60	36.28	0.6502
	2	1,200−2,300	0.9811	0.9177	0.8629	7.30	12.26	35.29	0.7784
	1	400−1,400	0.9088	0.9143	0.8577	8.52	12.59	36.25	0.8666
SNV	6	400−2,300	0.9351	0.8672	0.9396	3.93	8.07	23.24	0.0011
	6	**1,200−2,300**	**0.9630**	**0.8872**	**0.9311**	**6.87**	**8.81**	**25.37**	**0.1114**
	5	400−1,400	0.9011	0.8633	0.9222	11.94	2.21	28.55	2.60E^{-27}
Detrend	6	400−2,300	0.9424	0.8738	0.8370	8.13	13.35	38.46	1.98E^{-22}
	6	1,200−2,300	0.9767	0.8538	0.8846	13.58	11.95	34.42	1.79E^{-24}
	6	400−1,400	0.9255	0.7000	0.8242	9.21	13.94	40.14	1.15E^{-22}

*Supplementary VI. The calibration and validation sets of DHA contents by PLSR models from handheld-Raman spectra.*

| Data Pretreatment	Latent factors	Calibration set				Validation set			Sample
		Wavenumber (cm^{-1})	R^2 (model)	R^2 (cross validation)	R^2 (Pearson) Prediction	Bias	RSEP	RMSEP	p-value
No	9	400−2,300	0.9879	0.9273	0.9616	1.57	10.70	4.01	2.30E^{-10}
	8	1,200−2,300	0.9937	0.7711	0.9469	1.54	12.52	4.70	6.69E^{-21}
	7	400−1,400	0.9515	0.9090	0.9696	0.35	8.83	3.31	1.26E^{-18}
D1	4	400−2,300	0.9793	0.5159	0.7973	4.48	30.89	11.59	0.1778
	2	1,200−2,300	0.6822	0.1336	0.4607	6.26	42.96	16.12	1.31E^{-23}
	4	400−1,400	0.9589	0.7746	0.9288	3.56	19.21	7.21	3.54E^{-20}
D2	1	400−2,300	0.1837	0.0707	0.2912	4.59	46.32	17.38	3.51E^{-39}
	1	1,200−2,300	0.1926	0.0276	0.2808	4.59	46.14	17.41	1.41E^{-45}
	3	400−1,400	0.8050	0.1507	0.3144	7.23	45.96	17.24	1.09E^{-11}
Baseline	9	400−2,300	0.9879	0.9231	0.9616	1.57	10.07	4.01	2.27E^{-10}
	8	1,200−2,300	0.9937	0.8238	0.9469	1.54	12.52	4.70	6.72E^{-21}
	7	400−1,400	0.9515	0.9085	0.9696	0.35	8.83	3.31	1.26E^{-18}
OSC	**1**	**400−2,300**	**0.9455**	**0.9432**	**0.9778**	**0.35**	**7.97**	**2.99**	**0.5665**
	1	**1,200−2,300**	**0.9455**	**0.9450**	**0.9778**	**0.36**	**7.97**	**2.99**	**0.5649**
	1	**400−1,400**	**0.9456**	**0.9443**	**0.9778**	**0.35**	**7.97**	**2.99**	**0.5658**
SNV	8	400−2,300	0.9818	0.9222	0.9721	1.17	8.98	3.37	7.54E^{-08}
	9	1,200−2,300	0.9970	0.8557	0.9476	1.55	12.23	4.59	7.39E^{-11}
	7	400−1,400	0.9616	0.9327	0.9709	0.74	8.79	3.30	4.75E^{-18}
Detrend	7	400−2,300	0.9777	0.9287	0.9612	1.42	10.59	3.97	1.84E^{-10}
	5	1,200−2,300	0.9070	0.7842	0.9494	1.19	12.11	4.54	2.86E^{-20}
	6	400−1,400	0.9327	0.8958	0.9728	0.46	8.57	3.22	1.03E^{-19}

(A)

(B)

Supplement VII. Calibration curves of PLSR model (blue) and cross validation (red) of (A) PQ from handheld-Raman spectra (1,200–2,300 cm^{-1}) with SNV pretreatment and (B) DHA from handheld-Raman spectra (400–2,300 cm^{-1}) with OSC pretreatment.
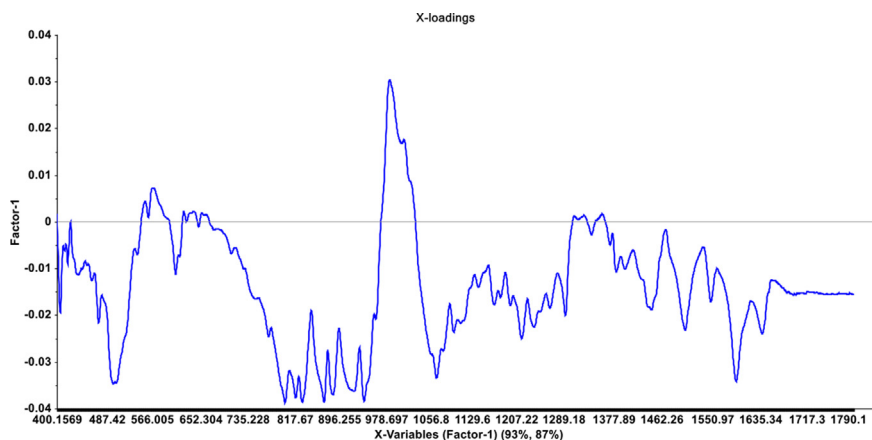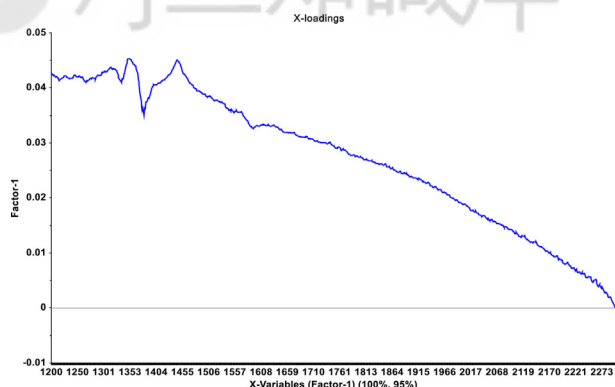

Supplement VIII. Loading plot of piperaquine (PQ) PLS model from FTIR data shows specific variables for the model and principle band around 1,550-1,680 cm^{-1} which correspond to C=C and C=N stretching in PQ structure.
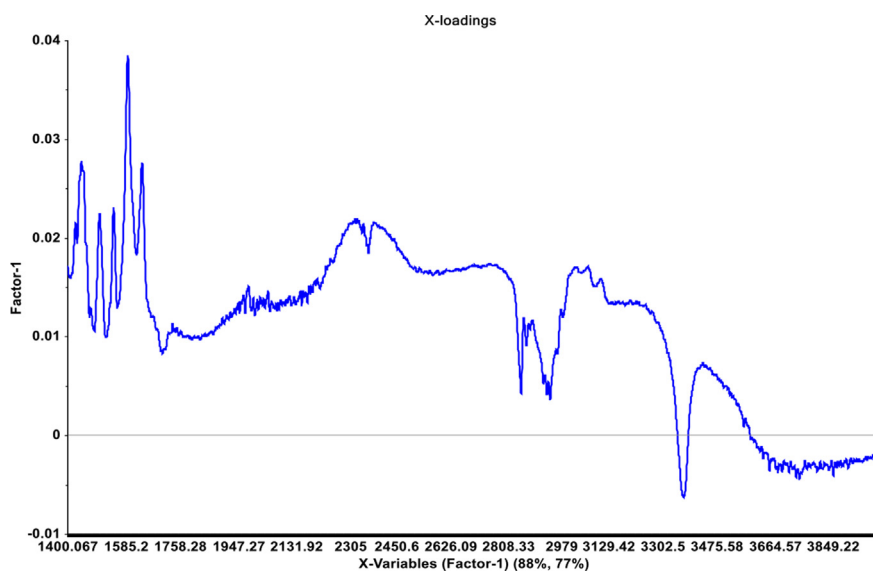
Supplement IX. Loading plot of dihydroartemisinin (DHA) PLS model from FTIR data shows specific variables for the model and principle band around 2,800−2,900 and 3,390 cm^{-1} which correspond to C−H stretching and -O-H stretching in DHA structure.
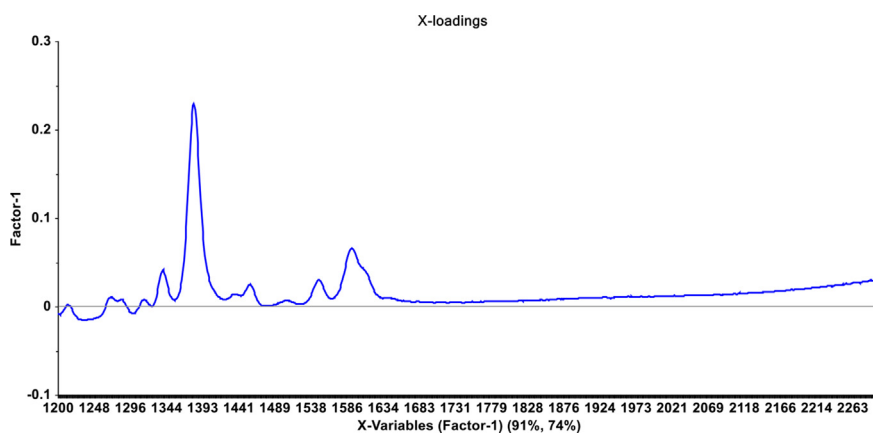
Supplement X. Loading plot of piperaquine (PQ) PLS model from handheld-Raman data shows specific variables for the model and principle band around 1,380 cm^{-1} which corresponds to aliphatic C−N stretching in PQ structure.

Supplement XI. Loading plot of dihydroartemisinin (DHA) PLS model from handheld-Raman data shows specific variables for the model and principle band around 1,380 cm^{-1} which corresponds to C−H bending in DHA structure.

References

[1] World Health Organization. World malaria report 2020: 20 years of global progress and challenges. Geneva, Switzerland: World Health Organization; 2020.

[2] World Health Organization. Guideline for treat malaria. 3rd ed. 2015. Italy.

[3] Davis T, Hung TY, Sim IK, Karunajeewa H, Ilett K. Piperaquine: a resurgent antimalarial drug. Drugs 2005;65: 75−87.

[4] Creek DJ, Bigira V, McCormack S, Arinaitwe E, Wanzira H, Kakuru A, et al. Pharmacokinetic predictors for recurrent malaria after dihydroartemisinin-piperaquine treatment of uncomplicated malaria in Ugandan infants. J Infect Dis 2013; 207:1646−54.

[5] Tarning J, Ashley EA, Lindegardh N, Stepniewska K, Phaiphun L, Day NP, et al. Population pharmacokinetics of piperaquine after two different treatment regimens with dihydroartemisinin-piperaquine in patients with Plasmodium falciparum malaria in Thailand. Antimicrob Agents Chemother 2008;52:1052−61.

[6] D'Acquarica I, Gasparrini F, Kotoni D, Pierini M, Villani C, Cabri W, et al. Stereodynamic investigation of labile stereogenic centres in dihydroartemisinin. Molecules 2010;15:1309−23.

[7] International pharmacopoeia 10th ed. Artenimol (artenimolum) monographs. Available at: https://digicollections.net/ phint/2020/index.html#d/b.6.1.29. [Accessed 20 September 2020].

[8] Guo YX, Zhang YJ, Ding T. Quantitative determination of piperaquine phosphate in dihydroartemisinin and piperaquine phosphate tablets by HPLC. J Chin Pharmaceut Sci 2008;43:713−4.

[9] Zhang Q, Li YF, Huang CZ. Quality control of piperaquine in pharmaceutical formulations by capillary zone electrophoresis. Talanta 2008;76:44−8.

[10] Lindegårdh N, White NJ, Day NP. High throughput assay for the determination of piperaquine in plasma. J Pharm Biomed Anal 2005;39:601−5.

[11] Chinh NT, Quang NN, Thanh NX, Dai B, Geue JP, Addison RS, et al. Pharmacokinetics and bioequivalence evaluation of two fixed-dose tablet formulations of dihydroartemisinin and piperaquine in Vietnamese subjects. Antimicrob Agents Chemother 2009;53:828−31.

[12] Chuvirasakul B, Joseph JF, Parr MK, Suntornsuk L. Development and applications of liquid chromatography-mass spectrometry for simultaneous analysis of anti-malarial drugs in pharmaceutical formulations. J Pharm Biomed Anal 2021:195. https://doi.org/10.1016/j.jpba.2020.113855. Available at: . [Accessed 20 September 2022].

[13] Deokate UA, Nawale RB, Gorde AM. Development and validation of RP-HPLC method for simultaneous estimation of piperaquine phosphate and dihydroartemisinin in bulk. Int J Pharm Pharmaceut Sci 2014;6:441−4.

[14] Matthias O. Chemometrics: statistics and computer application in analytical chemistry. 3rd ed. 2017. Germany. Weinhem.

[15] Chemistry libretexts. Infrared spectroscopy. 2020. Available at: https://chem.libretexts.org/%20go/page/1847. [Accessed 14 March 2021].

[16] Ausili A, Sánchez M, Gómez-Fernández J. Attenuated total reflectance infrared spectroscopy: a powerful method for the simultaneous study of structure and spatial orientation of lipids and membrane proteins. Biomed Spectrosc Imag 2015; 4:159−70.

[17] Bumbrah GS, Sharma RM. Raman spectroscopy − basic principle, instrumentation and selected applications for the characterization of drugs of abuse. Egypt J Forensic Sci 2016; 6:209−15.

[18] Monica B, Simion A, Traian I. Raman and SERS investigations of pharmaceuticals. Germany: Berlin; 2008.

[19] Boyer C, Gaudin K, Kauss T, Gaubert A, Boudis A, Verschelden J. Development of NIRS method for quality control of drug combination artesunate-azithromycin for the treatment of severe malaria. J Pharm Biomed Anal 2012;67−68:10−5.

[20] Teixeira KSS, da Cruz Fonseca SG, de Moura LCB, de Moura MLR, Borges MHP, Barbosa EG. Use of chemometrics to compare NIR and HPLC for the simultaneous determination of drug levels in fixed-dose combination tablets employed in tuberculosis treatment. J Pharm Biomed Anal 2018;149:557−63.

[21] Marson BM, de Oliveira Vilhena R, de Souza Madeira CR, Pontes FLD, Piantavini MS, Pontarolo R. Simultaneous quantification of artesunate and mefloquine in fixed-dose combination tablets by multivariate calibration with middle infrared spectroscopy and partial least squares regression. Malar J 2016;15:109−16.

[22] Guimaraes L, Parada Moreira L, Lourenço B, Toma W, Zângaro R, Pacheco M. Multivariate method based on Raman spectroscopy for quantification of dipyrone in oral solutions. J Spectrosc 2018;40:1−10.

[23] ICH guideline. Q2 (R1) validation of analytical procedure: text and methodology. Available at: https://database.ich.org/ sites/default/files/ICH_Q2-R2_Document_Step2_Guideline _2022_0324.pdf. [Accessed 24 October 2022].

[24] National Institute of Standards and Technology. Central composite designs (CCD). Available at: https://www.itl.nist. gov/div898/handbook/pri/section3/pri3361.htm. [Accessed 21 January 2021].

[25] Develve. Central composite design. Available at: https:// develve.net/Central%20 Composite%20design.html. [Accessed 21 January 2021].

[26] Jun H, Saly RT, Mojgan M. Practical considerations in data pretreatment for NIR and Raman spectroscopy American pharmaceutical review. Available at: https://www. americanpharmaceuticalreview.com/Specialty/Drug_ Delivery/Featured-Articles/116330-Practical-Considerations-in-Data-Pretreatment-for-NIR-and-Raman-Spectroscopy/. [Accessed 21 January 2021].

[27] Esquerre C, Gowen AA, Burger J, Downey G, O'Donnell CP. Suppressing sample morphology effects in near infrared spectral imaging using chemometric data pretreatments. Chemometr Intell Lab Syst 2012;117:129−37.

[28] Liland KH, Rukke E-O, Olsen EF, Isaksson T. Customized baseline correction. Chemometr Intell Lab Syst 2011;109:51−6.

[29] Niazi A, Azizi A, Ramezani M. Simultaneous spectrophotometric determination of mercury and palladium with Thio-Michler's Ketone using partial least squares regression and orthogonal signal correction. Spectrochim Acta Mol Biomol Spectrosc 2008;71:1172−7.

[30] Fearn T, Riccioli C, Garrido-Varo A, Guerrero-Ginel JE. On the geometry of SNV and MSC. Chemometr Intell Lab Syst 2009;96:22−6.

[31] Liu Y, Liu Y, Chen Y, Zhang Y, Shi T, Wang J. The influence of spectral pretreatment on the selection of representative

calibration samples for soil organic matter estimation using vis-NIR reflectance spectroscopy. Rem Sens 2019;11:1−16.

[32] Biancolillo A, Marini F. Chemometric methods for spectroscopy-based pharmaceutical analysis. Front Chem 2018;6:576−89.

[33] Kumar N, Bansal A, Sarma GS, Rawal RK. Chemometrics tools used in analytical chemistry: an overview. Talanta 2014; 123:186−99.

[34] Avery IM. The Jackknife estimation method. Available at: https://arxiv.org/pdf/1606.00497.pdf#:~:text=The% 20JackknifeEstimation%20Method%20Avery%20I.% 20McIntosh%20The%20empirical,%28CDF%29%20from% 20which%20the%20samples%20were%20drawn%2C%20F. [Accessed 10 March 2021].

[35] Htet TT, Cruz J, Khongkaew P, Suwanvecho C, Suntornsk L, Nuchtavorn N, et al. PLS-regression-model-assisted Raman spectroscopy for vegetable oil classification and non-destructive analysis of alpha-tocopherol contents of vegetable oils. J Food Compos Anal 2021:103. https://doi.org/ 10.1016/j.jfca.2021.104119. Available at:　　 [Accessed 22 September 2022].

[36] Bland JM, Altman DG. Statistical methods for assessing agreement between two methods of clinical measurement. Lancet 1986;327:307−10.

[37] Giavarina D. Understanding Bland altman analysis. Biochem Med 2015;25(2):141−51.